


Article

Effect of Sorbitol Templates on the Preferential Crystallographic Growth of Isotactic Polypropylene Wax

Zoe V. Quiñones-Jurado ¹ , Carlos A. Ávila-Orta ² , Blanca E. Castillo-Reyes ¹,
José M. Mata-Padilla ², Benjamin S. Hsiao ³, Francisco J. Medellín-Rodríguez ^{3,*}
and Miguel A. Waldo-Mendoza ^{1,*} 

- ¹ Innovación y Desarrollo en Materiales Avanzados A. C., Grupo POLYnnova, Carr. San Luis Potosí-Guadalajara 1510, Nivel 3, Local 12, Lomas del Tecnológico, San Luis Potosí 78211, Mexico; zoe.vineth@polynnova.mx (Z.V.Q.-J.); becr_iq@yahoo.com.mx (B.E.C.-R.)
- ² Centro de Investigación en Química Aplicada, Blvd. Ing. Enrique Reyna H. 140, Col. San José de los Cerritos, Saltillo, Coahuila 25294, Mexico; carlos.avila@ciqa.edu.mx (C.A.Á.-O.); jose.mata@ciqa.edu.mx (J.M.M.-P.)
- ³ Department of Chemistry, Stony Brook University, Stony Brook, NY 11794-3400, USA; benjamin.hsiao@stonybrook.edu
- * Correspondence: francisco.medellin@stonybrook.edu (F.J.M.-R.); miguel.waldo@polynnova.mx (M.A.W.-M.); Tel.: +1-631-632-5793 (F.J.M.-R.); +52-444-870-0700 (M.A.W.-M.)

Received: 19 November 2017; Accepted: 22 January 2018; Published: 26 January 2018

Abstract: The crystallization of isotactic polypropylene wax (iPP) in the presence of different sorbitol structures was studied. Dibenzylidene Sorbitol (DBS), as well as two of its derivatives with one or two methyl groups in the DBS molecule (MDBS and DMDBS, respectively), were tested as nanometer-size fibrillar templates. The early nucleation stage and crystal morphology were analyzed in Real-Time Wide-Angle X-ray Scattering (WAXS) and polarized optical microscopy (POM). It was found that the iPP crystals showed an α -phase unit cell for the three different sorbitols. However, a preferential crystal growth in the plane (040) was observed for iPP–MDBS. The macrostructure morphology of the iPP–DBS and iPP–DMDBS wax compounds was spherulitic, while nodular macrocrystals were observed for the iPP–MDBS compound. It was concluded that the MDBS template promoted a lower interface energy because of its match with the c-axis of the iPP wax crystals, whereas, in the case of the DBS and DMDBS templates, the preferential plane was the (110), characteristic of the iPP spherulitic arrangement.

Keywords: template; crystal growth; sorbitol; isotactic polypropylene wax; preferential arrangement

1. Introduction

The formation of crystals during the solidification or annealing of semicrystalline polymers provides superior properties such as mechanical strength, dimensional stability, optical control, gas barrier, and shorter molding times [1,2]. Semicrystalline isotactic polypropylene (iPP) is a widely used polymer because of its improved mechanical properties compared with its atactic and syndiotactic forms, and it can replace other expensive engineering thermoplastics [3].

iPP self-organizes into a spherulitic morphology when crystallizing in the absence of external forces or additives [4]. However, in the presence of external forces or additives, other macrostructures have been reported such as cylindrites, axialites, quadrites, hedrites, dendrites, and nodular and shish kebab [5–7]. These macrostructures are constituted of crystal unit cells which can be monoclinic (α -iPP), hexagonal (β -iPP), triclinic (γ -iPP), or in a smectic phase [8]. Although it is infrequent, the simultaneous

presence of two polymorphs can also occur during iPP crystallization [9]. α -iPP crystals are frequently found under normal processing conditions [10]. Some nucleating agents, as well as mechanical stress, induce the formation of β -iPP crystals [11]. γ -iPP crystals can be obtained for samples with low molecular weight, low tacticity, copolymers (metallocene catalysts), and also when elevated pressures and high temperature are used (degraded samples) [12]. Finally, the smectic or mesomorphic crystals can be obtained at high cooling rates [13]. The concomitant crystallization of α -iPP and β -iPP crystals has been reported in the presence of small amounts of β -nucleants (0.01–0.5 wt. %), such as calcium pimelate [14]. In the neat polymer, the concomitant crystallization can occur if the crystallization is carried out using a temperature gradient, melt crystallization between 110–140 °C, or under shear flow [15]. Cocrystallization has also been reported at conditions above 75 MPa, 140 °C, and for the crystallization of metallocene iPP [15].

The crystal type and macrostructure morphology of iPP depend strongly on the nucleation process. Dibenzylidene sorbitol (DBS) has been widely used as a nucleating agent to crystallize iPP [16–18]. Recently, this compound has attracted increased attention due to the fact that controlled nanometer-size templates can be obtained [19,20]. Lipp et al. showed that some sorbitols are suitable to form nanofibrillar structures that are able to reduce the free energy barrier to nucleate iPP [21]. Moreover, Shepard et al. described that the DBS molecules can self-organize into fibers with a diameter of ca. 10 nm through hydrogen bonding, where the interaction of acetal oxygens and pendant hydroxyl groups of the phenyl rings in the sorbitol structure provides cleft interfaces adequate to stabilize the polypropylene helix and avoid the return to the random-coil conformation [22]. Besides, Smith et al. reported that DBS sorbitol molecules provide stabilization and minimize the steric clashes of the methyl groups of iPP [23]. The methyl groups can be bonded to DBS to obtain DBS derivatives such as methyl dibenzylidene sorbitol (MDBS) and dimethyl dibenzylidene sorbitol (DMDBS). The molecular structures of DBS and its derivatives are shown in Figure 1.

iPP waxes are used to aid the processing of iPP polymers, as well as to assist the dispersion in iPP-based compounds. Therefore, it is important to understand the effect of the DBS fibers and their derivatives as templates in the crystallization, crystal structure, and morphology of the iPP wax. For this purpose, wide-angle X-ray scattering (WAXS) patterns were obtained in real time using synchrotron light in order to determine the crystal structure evolution with time. Polarized optical microscopy (POM) was used to determine the growth rate and crystalline macrostructure morphology of iPP.

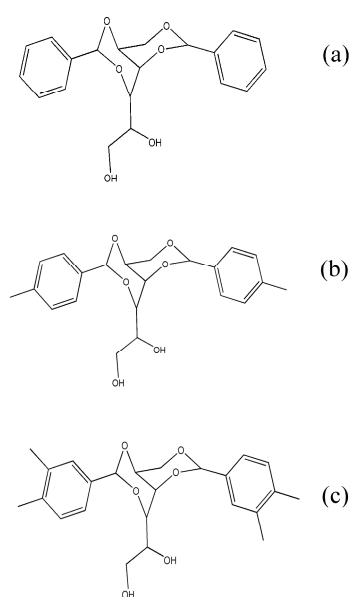


Figure 1. Sorbitol molecules used in this work: (a) DBS, (b) MDBS, and (c) DMDBS.

2. Materials and Methods

2.1. Materials and Sample Preparations

The isotactic metallocene polypropylene wax of average $M_w \sim 12,000$ and $M_n \sim 5000$ g/g-mol, with an experimentally determined isotacticity index of 92.25% (ASTM D5492-98) was obtained from Aldrich (St. Louis, MO, USA). The iPP wax was used as received. The nucleating agents 1,3:2,4-dibenzylidene sorbitol (DBS), 1,3:2,4-bis(*p*-methylbenzylidene) sorbitol (MDBS), and bis(3,4-dimethylbenzylidene) sorbitol (DMDBS) were obtained from Milliken Chemical (Ghent, Belgium). In order to eliminate the moisture content, all the nucleating agents were dried in an oven at 60 °C for 3 h prior to mixing with the iPP wax. The blends of iPP with the sorbitol agents at the concentrations of 0.02–0.2 wt. % were prepared by melt mixing of the components at a temperature of 280 °C, under constant stirring for 7 min. Also, antioxidants obtained from CIBA (Basel, Switzerland) (0.08 ppm Irgafos-168 and 0.04 ppm of Irganox-1010) were used during melt mixing.

2.2. Differential Scanning Calorimetry

The efficiency of the nucleating additives in iPP under dynamic differential calorimetry was determined considering the change in enthalpy (ΔH) originated during iPP crystallization. The crystallization and melting behavior of the pure polymer and the three iPP–sorbitol compounds was studied using a Perkin Elmer DSC (Pyris 7). The melting temperature (T_m) and crystallization temperature (T_c), were determined on samples with weight ranging from 5 to 10 mg in a nitrogen atmosphere with a heating and cooling rate of 10 °C/min. The samples were preliminarily heated to 187.5 °C and held isothermally for 3 min to eliminate residual crystals.

2.3. Polarized Optical Light Microscopy

The heating process of the isothermally crystallized samples was monitored in situ using an Olympus BX60 transmission optical microscope with crossed polars and a 20X objective (resolution of 1.84 mm). The microscope was coupled to a Mettler FP82HT hot stage controlled by an FP90 digital controller to keep the isothermal crystallization temperature at 135 °C.

2.4. Real-Time Wide Angle X-ray Scattering (WAXS)

Real-Time X-ray Wide-Angle Scattering experiments were performed at the X27C beamline of the National Synchrotron Light Source (Brookhaven National Laboratory, Upton, NY, USA). For this purpose, two-dimensional patterns were first obtained and then computer subtracted in order to obtain the X-ray scattering pattern. The sample to detector distance was 125.5 mm. The patterns were corrected for set up conditions, and the scattering was calibrated with aluminum oxide as a standard. The wavelength of the X-ray beam was 1.366 Å, and a three-pinhole collimator system was used to reduce the beam size to 0.6 mm in diameter.

3. Results and Discussion

3.1. Thermal Behavior of iPP Wax and Nucleating Agents

The nucleating agents and the iPP wax were thermally characterized by DSC analysis to find the temperature range of miscibility. Figure 2a shows the DSC traces of the iPP wax, DBS, MDBS, and DMDBS during heating up to 280 °C. The temperature at the endothermic peak were used to determine the melting point, and the values obtained were 155.5, 228.7, 260.7, and 271.6 °C, respectively. Thus, the temperature chosen to blend the compounds was 280 °C, aiming to maintain in a molten state the different nucleating agents as well as the iPP wax. Besides, in Figure 2b it can be observed that sorbitols crystallize during cooling from the molten state at a higher temperature than the iPP wax. Therefore, the temperature of 135 °C was chosen to crystallize the iPP wax, so that sorbitol fibrils remained as an interphase template. It is well known that sorbitols can create nanometer-size fibrils

because of the intramolecular interactions of the acetal groups, in such a way that the growth of these fibrils leads to a three-dimensional network, where their size is dependent on the concentration [24].

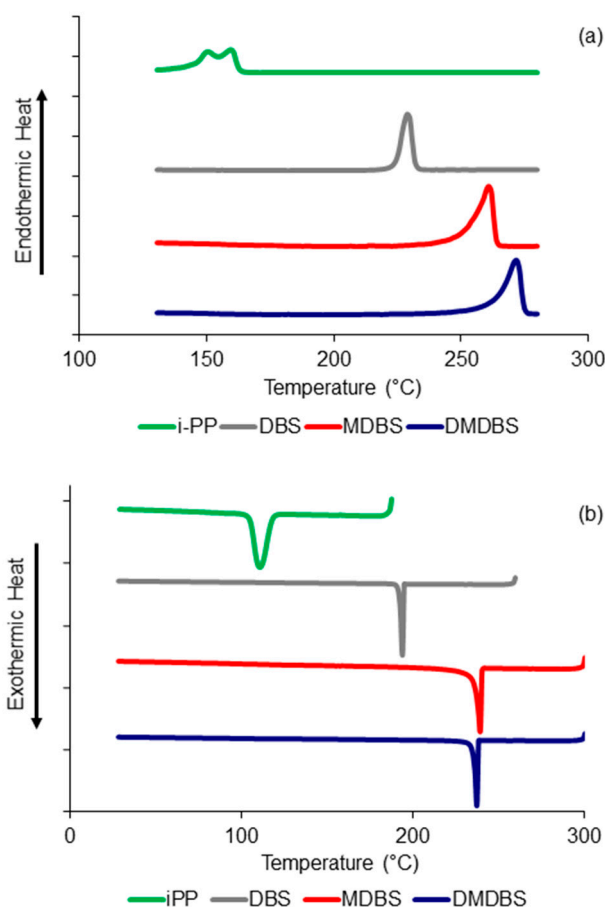


Figure 2. Thermal properties of the studied materials: (a) melting points and (b) crystallization temperatures of the iPP wax and nucleating agents (heat and cooling rates of 10 °C/min).

3.2. Sorbitol Nucleating Effect on iPP Wax

The use of micrometric sorbitol fibrils as a nucleating agent to crystallize propylene is well known. For industrial purposes, the minimum concentration of sorbitol is established that allows the maximum crystallization efficiency. However, the effect of the structures at their nanometric level has not yet been tackled. The use of these fibrillar structures as nanometric templates opens the possibility of having a better control on the nucleation performance of such sorbitol agents. For this reason, in this study, a minimum concentration of the sorbitol agent was required to establish the concentration where a significant difference in crystallization activity occurs, in order to avoid the formation of microaggregates.

The size of the fibrillar substrate depends on the sorbitol concentration; therefore, the nucleation saturation was first determined. The nucleating effect on the iPP wax for the different sorbitols used in this study is shown in Figure 3. This effect is referred to the crystallization temperature as a function of sorbitol concentration. The crystallization temperature of the iPP wax nucleated with sorbitol molecules mono- and disubstituted with methyl pendant groups was higher than that obtained for the simple structure DBS. The effect on the iPP wax crystallization at the concentration of 0.02 wt. % was identical for all cases, with $T_c = 111.9$ °C. However, at the concentration of 0.04 wt. %, a stronger nucleating effect was presented by MDBS ($T_c = 118.7$ °C), followed by DMDBS ($T_c = 113.7$ °C), and DBS ($T_c = 112.4$ °C). Finally, MDBS and DMDBS exhibited a nucleating maximum at the concentration of

0.1 wt. %, whereas DBS showed a shift to a higher temperature at the concentration of 0.2 wt. %. In this regard, the concentration of 0.04 wt. % was used hereinafter, since it is expected that the smallest possible size of fibrillary network can be obtained at this concentration, which thus is suitable for the evaluation of the ability of different sorbitol structures to modify the morphology of the iPP wax.

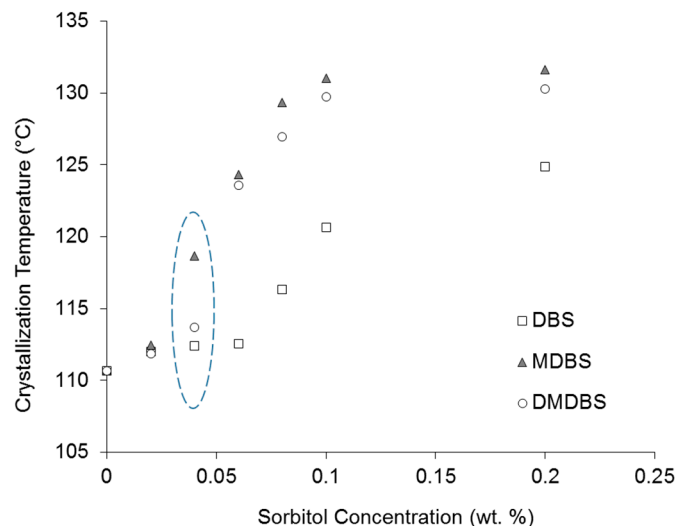


Figure 3. Efficiency of sorbitol nucleating effect in the iPP wax at the concentration of 0.02, 0.04, 0.06, 0.08, 0.1, and 0.2 wt. % of DBS, MDBS, and DMDBS.

3.3. Unit Cells and Lamellar Structures during Isothermal Crystallization

The evolution of the crystal structure unit cell of iPP in the presence of sorbitol derivatives was determined by Real-Time WAXS. Figure 4 shows the diffraction peaks of the iPP wax crystals, during in situ isothermal crystallization at 135 °C. The WAXS pattern after 40 min of isothermal crystallization showed diffraction peaks corresponding to the crystallographic planes (110), (040), (130), (111)/(041), and (060) of the α -iPP phase. It is noticeable that the growth of the crystallographic planes appeared in different times and surprisingly in a different sequence, depending on the sorbitol structure. The chain arrangement of the iPP wax blended with the DBS and DMDBS fibrillar networks indicating that, in the early crystallization stages, the wax amorphous phase was transformed to form the crystallographic plane (110), which appeared after 10 min of thermal treatment. Subsequently, other diffraction peaks emerged. All peaks were present after 15 min in the presence of DMDBS and after 20 min with DBS. The intensity of the diffraction peak of the (110) crystallographic plane, which can be related to the angle in the monoclinic unit cell of the α -iPP crystals, confirms the growth of daughters on mother lamellae [25]. On the other hand, the iPP wax nucleated faster in the presence of the MDBS structure, thus the crystal growth was faster than in the presence of the other sorbitol substrates. Moreover, it was evident that the diffraction plane (040) appeared at an early stage in the presence of MDBS, even only after 6 min of isothermal crystallization (Figure 4). Besides, the intensity level of the diffraction peak (040) competed with the intensity of the diffraction peak (110). This behavior could be similar to the transcrystallization process developed during the epitaxial growth of iPP with reinforcement particles and fibers [26], where the (040) plane enhancement was associated with highly oriented structures [27].

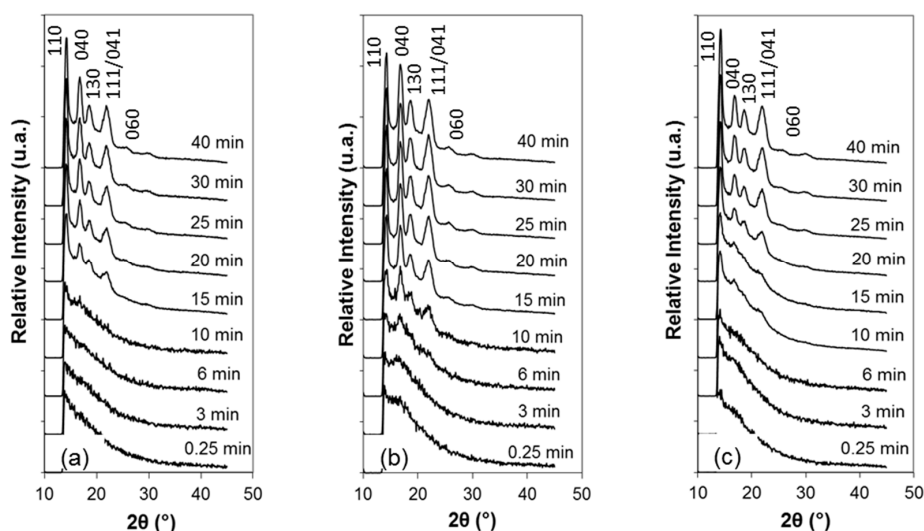


Figure 4. RT-WAXS patterns of the iPP wax-sorbitol compounds during in situ crystallization at 135 °C; (a) iPP wax-DBS, (b) iPP wax-MDBS and (c) iPP wax-DMDBS.

3.4. Macrostructure Morphology during Isothermal Crystallization

To visualize the growth rate and the formation of the crystalline macrostructure of the iPP wax due to the effect of the heterogeneous nucleation using sorbitols, polarized light optical microscopy was used. The crystal development of the iPP wax using 0.04 wt. % of nucleating agent at 135 °C allowed the analysis of the transformation from the amorphous to the crystalline phase of the iPP wax on sorbitol fibrillar templates as a result of the low nucleation rate. It was observed that sorbitol molecules act as an effective nucleating agent, even at the low concentration level of 0.04 wt. % (Figure 5). The micrographs indicated that the iPP wax-sorbitol compound had different crystallization rates for both stages of nucleation and of crystal growth, with MDBS > DMDBS > DBS (Figures 5 and 6). The DBS and DMDBS substrates promoted the formation of iPP wax crystalline embryos at 5 min, while a faster rate was determined for the iPP wax-MDBS compound (Figure 6), i.e., the nuclei appeared at 1 min, and crystal growth was completed in 15 min. Additionally, the morphology of the iPP wax-MDBS compound was not isotropic and was different from the characteristic spherulites. The macrostructure shape of this compounds occurred in the form of elongated nodules. To determinate and corroborate this change in the geometric crystal growth, the Avrami index was calculated using the transmitted light intensity vs time curves obtained from the POM analysis (Figure 6) [28]. The results are shown in Table 1, while the corresponding Avrami parameter of the neat polymer wax did not occur within the frame time of the experiment. The Avrami index of 1.95 for the iPP-MDBS compound was found and indicated that the growth was two-dimensional ($n = 2$, Disk). On the other hand, the use of DBS or DMDBS resulted in a higher Avrami index ($n = 3$) that corresponded to the radial growth of the iPP lamellae in a random direction. Unlike the geometric growth ($n = 2$), the growth of spherulites ($n = 3$) is a typical morphology reported for iPP-DMDBS when it is crystallized at $T_c = 135$ °C [29] and at a low nucleating content (0.22, 0.31, and 0.52 wt. %) [30].

Table 1. Avrami index of wax crystallization using sorbitol templates.

Sorbitol Template	Avrami Index (n)	Crystal Geometry
DBS	3.11	Spherulitic
MDBS	1.95	Disk
DMDBS	2.96	Spherulitic

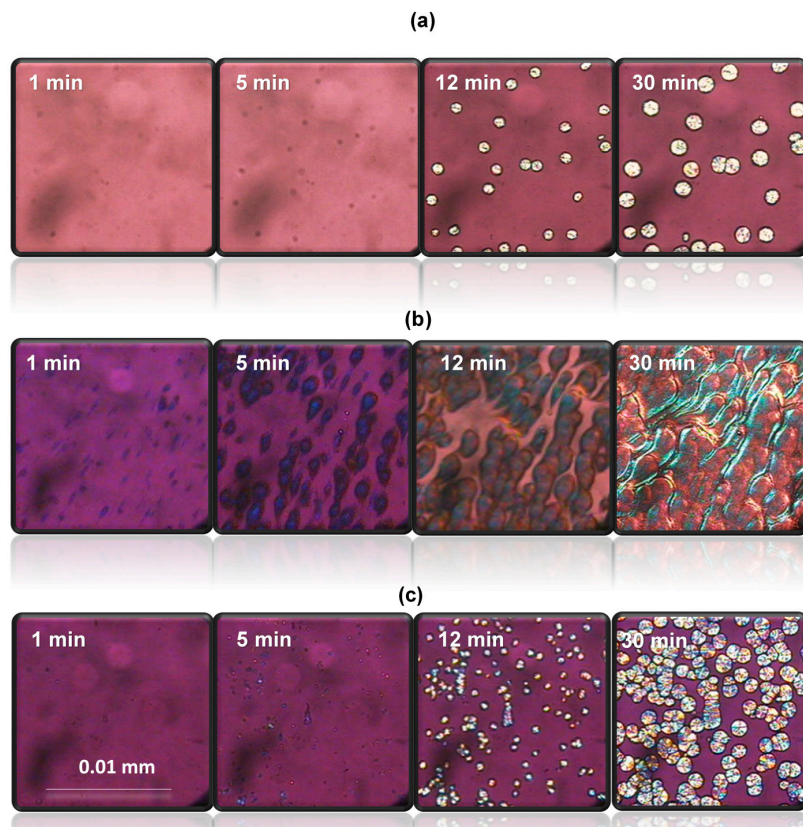


Figure 5. Polarized optical micrographs of the isothermal crystallization at 135 °C for the iPP wax-sorbitol compounds; (a) DBS, (b) MDBS, and (c) DMDBS, for 1 min, 5 min, 12 min and 30 min, respectively, left to right.

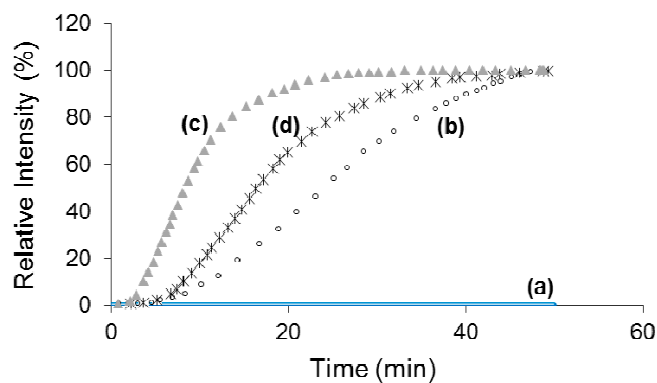


Figure 6. Transmitted light intensity during the isothermal crystallization at 135 °C for (a) iPP wax and wax-sorbitol compounds; (b) DBS, (c) MDBS, and (d) DMDBS.

3.5. Interfacial Crystallization of the iPP Wax-Sorbitol Compounds

The X-ray and optical microscopy analyses supported an improvement of the interfacial interaction between the iPP wax chains and the sorbitol substrates, because of the lower interface energy which resulted in a faster crystallization process.

The macrostructure in the iPP-DBS and iPP-DMDBS wax compounds was spherulitic. Figure 7a schematizes that these templates developed nucleation sites that resulted in isotropic polycrystalline aggregates, because the lamellas could freely organize without restriction during the radial growth. According to Shepard et al., the nucleation is due to the stabilization of the helix projection of iPP [22],

which would promote the best match of the templates (DBS and DMDBS) with the b-axis of the iPP wax chains.

On the other hand, an anisotropic crystalline macrostructure (Figure 7b) was developed for the iPP–MDBS wax compound. It is important to note that the MDBS template presented a low interface energy, which led to both the nonconventional arrangement of polycrystalline aggregates and to the enhancement of the crystallization rate. In this case, a disk-like crystal growth mode was confirmed by the corresponding Avrami exponent (closer to $n = 2$). Another important performance of the MDBS template was that the crystalline iPP wax showed preferential diffraction from the plane (040), as commonly occurs for transcrystallization, i.e., crystal orientation is due to the formation of row nuclei along the fibers or other interfaces [27,31]. This was probably due to a high density of nuclei imposed on this template resulting in confined crystal growth. A scheme of the MDBS template match with the c-axis of the iPP wax crystals is shown in Figure 7. The match improved the stabilization of the polypropylene methyl group between the cleft interfaces into the fibrillar template.

The main industrial application of sorbitol is as an additive to promote the optical clarity and aesthetic appeal of polypropylene films. However, the mechanical properties can be affected because of the crystal structure and macrostructure morphology of the iPP wax resulting from the interaction with DBS-based templates. In this study, the development of an interesting crystalline structure of the iPP wax using MDBS as a template was observed, in which α -iPP crystals showed preferential growth in the crystal plane (040) resulting in an anisotropic elongated nodulus. This microstructure can be related to an increase in mechanical properties. For example, Amitay-Sadovsky et al. reported the increase in the shear modulus as a result of an increase of crystal anisotropy in a nanoindentation study [32].

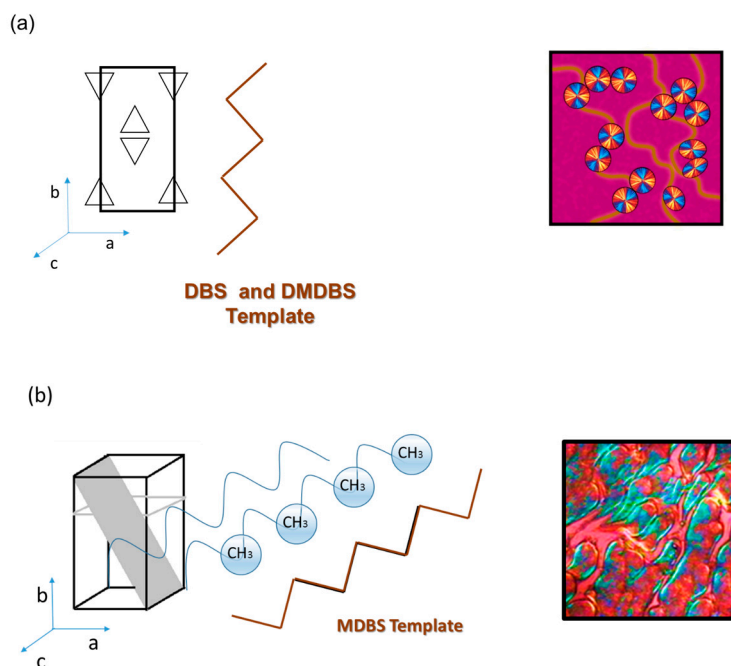


Figure 7. Scheme of the stabilization of a polypropylene wax between the cleft interfaces of the fibrillar templates. Interface match with sorbitol templates: (a) stabilization by match with the helix of the iPP wax, of DBS, or DMDBS, and (b) stabilization by match with the methyl groups of MDBS.

4. Conclusions

The iPP crystallization was accelerated by the DBS Sorbitol and alkylated derivatives at very low concentrations. MDBS and DMDBS exhibited a nucleating maximum at the concentration of 0.1 wt. %, whereas DBS reached the threshold concentration of nucleating at 0.2 wt. %. The minimum

concentration of the sorbitol structures that delimited the rate of crystallization was 400 ppm. Under the isothermal treatment at 135 °C, all the iPP–sorbitol compounds showed α -iPP crystals. The growth rate of crystallization of the iPP–MDBS compound was higher than that of the DBS or DMDBS compounds. Particularly, the dibenzylidene sorbitol substrates acted as crystallization templates on the polymer chains, which resulted in a different geometry of the iPP molecular macrostructures. The crystallization process monitored in real time by POM and WAXS confirmed the crystal evolution and the preferential crystallographic growth. In the presence of the DBS and DMDBS substrates, the iPP amorphous phase was transformed to form the crystallographic plane (110), resulting in spherulite-like crystals. For the iPP–MDBS compound, the intensity level of the (040) reflection competed with the (110) reflection, because MDBS behaved as a template able to nucleate iPP, resulting in a transcrystal-like behavior. In this case, a greater stabilization of the polypropylene methyl group between the cleft interfaces of the fibrillar template took place.

Author Contributions: Zoe Vineth Quiñones-Jurado measured POM and DSC experiments and wrote the paper, Carlos A. Ávila-Orta provided technical discussions and revised the final version of the paper, Blanca E. Castillo-Reyes prepared and characterized the polypropylene-sorbitol blends, José M. Mata-Padilla analyzed optical and thermal results, Benjamin S. Hsiao provided technical discussions, Francisco J. Medellín-Rodríguez provided technical discussions and reviewed and contributed to the final revised manuscript and Miguel A. Waldo-Mendoza conceived the paper, revised and approved the final version. Measured Real-Time WAXS experiments.

Conflicts of Interest: The authors declare no conflict of interest.

References

- Smith, T.L.; Masilamani, D.; Bui, L.K.; Brambilla, R.; Khanna, Y.P.; Garbriel, K.A. Acetals as nucleating agents for polypropylene. *J. Appl. Polym. Sci.* **1994**, *52*, 591–596. [[CrossRef](#)]
- Bernland, K.; Goossens, J.G.P.; Smith, P.; Tervoort, T.A. On clarification of haze in polypropylene. *J. Polym. Sci. Part B Polym. Phys.* **2016**, *54*, 865–874. [[CrossRef](#)]
- Fairgrieve, S. *Nucleating Agents*, 1st ed.; Rapra Technology, Rapra Review Report 187, SPF Polymer Consultants; iSmithers Rapra Publishing: Shawbury, UK, 2005; Volume 16, p. 6.
- Lin, K.-Y.; Xanthos, M.; Sirkar, K.K. Novel polypropylene-based microporous membranes via spherulitic deformation. *J. Membr. Sci.* **2009**, *330*, 267–278. [[CrossRef](#)]
- Folkes, M.J. Interfacial crystallization of polypropylene in composites. In *Polypropylene: Structure, Blends, and Composites*, 1st ed.; Karger-Kocsis, J., Ed.; Chapman and Hall: London, UK, 1995; Volume 3, p. 340.
- Wang, X.; Ouyang, J.; Su, J.; When, Z. Investigating the role of oriented nucleus in polymer shish-kebab crystal growth via phase-field method. *J. Chem. Phys.* **2004**, *140*, 114102. [[CrossRef](#)] [[PubMed](#)]
- Qiu, J.; Wang, Z.; Yang, L.; Zhao, J.; Niu, Y.; Hsiao, B. Deformation-induced highly oriented and stable mesomorphic phase in quenched isotactic polypropylene. *Polymer* **2007**, *48*, 6934–6947. [[CrossRef](#)]
- Bruckner, S.; Meille, S.V.; Petraccone, V.; Pirozzi, B. Polymorphism in isotactic polypropylene. *Prog. Polym. Sci.* **1991**, *16*, 361–404. [[CrossRef](#)]
- Fischer, C.; Drummer, D. Crystallization and Mechanical Properties of Polypropylene under Processing-Relevant Cooling Conditions with Respect to Isothermal Holding Time. *Int. J. Polym. Sci.* **2016**, *2016*, 1–11. [[CrossRef](#)]
- Turner-Jones, A.; Aizlewood, J.M.; Beckett, D.R. Crystalline forms of isotactic polypropylene. *Makromol. Chem.* **1964**, *75*, 134–158. [[CrossRef](#)]
- Varga, J. β -Modification of isotactic polypropylene: Preparation, structure, processing, properties, and application. *J. Macromol. Sci. B* **2002**, *41*, 1121–1171. [[CrossRef](#)]
- Sowinski, P.; Piorkowska, E.; Boyer, S.; Haudin, J. Nucleation of crystallization of isotactic polypropylene in the gamma form under high pressure in nonisothermal conditions. *Eur. Polym. J.* **2016**, *85*, 564–574. [[CrossRef](#)]
- Ma, Z.; Shao, C.G.; Wang, X.; Zhao, B.J.; Li, X.Y.; An, H.N.; Yan, T.Z.; Li, Z.M.; Li, L.B. Critical stress for drawing-induced alpha crystal-mesophase transition in isotactic polypropylene. *Polymer* **2009**, *50*, 2706–2715. [[CrossRef](#)]

14. Looijmans, S.; Menyhard, A.; Peters, G.; Alfonso, G.; Cavallo, D. Anomalous temperature dependence of isotactic polypropylene α -on- β cross-nucleation kinetics. *Cryst. Growth Des.* **2017**, *17*, 4936–4943. [[CrossRef](#)]
15. Dou, Q.; Xue, J. Effect of an In-Situ Nucleating Agent on the Polymorphs and Mechanical Properties of Isotactic Polypropylene. *J. Macromol. Sci. B* **2015**, *54*, 947–961. [[CrossRef](#)]
16. Suzuki, M.; Hanabusa, K. Polymer organogelators that make supramolecular organogels through physical cross-linking and self-assembly. *Chem. Soc. Rev.* **2010**, *39*, 455–463. [[CrossRef](#)] [[PubMed](#)]
17. Balzano, L.; Rastogi, S.; Gerrit, W.M. Flow Induced Crystallization in Isotactic Polypropylene–1,3:2,4-Bis (3,4-dimethylbenzylidene)sorbitol Blends: Implications on Morphology of Shear and Phase Separation. *Macromolecules* **2008**, *41*, 399–408. [[CrossRef](#)]
18. Okesola, B.; Vieira, V.; Cornwell, D.; Whitelaw, N.; Smith, D. 1,3:2,4-Dibenzylidene-D-sorbitol (DBS) and its derivatives—Efficient, versatile and industrially-relevant low-molecular-weight gelators with over 100 years of history and a bright future. *Soft Matter* **2015**, *11*, 4768–84787. [[CrossRef](#)] [[PubMed](#)]
19. Wang, D.; Zhang, X.; Liu, Y.; Li, L.; Bo, Z.; Zhou, J.; Huo, H. Structure difference of sorbitol derivatives influence the crystallization and performance of P3OT/PCBM organic photovoltaic solar cells. *Org. Electron.* **2017**, *46*, 158–165. [[CrossRef](#)]
20. Lai, W.; Tseng, S.; Chao, Y. Effect of Hydrophobicity of Monomers on the Structures and Properties of 1,3:2,4-Dibenzylidene-d-sorbitol Organogels and Polymers Prepared by Templating the Gels. *Langmuir* **2011**, *27*, 12630–12635. [[CrossRef](#)] [[PubMed](#)]
21. Lipp, J.; Shuster, M.; Terry, A.E.; Cohen, Y. Fibril formation of 1,3:2,4-Di(3,4-dimethylbenzylidene) sorbitol in polymer melts. *Polym. Eng. Sci.* **2008**, *48*, 705–710. [[CrossRef](#)]
22. Shepard, T.A.; Delsorbo, C.R.; Louth, R.M.; Walborn, J.L.; Norman, D.A.; Harvey, N.G.; Spontak, R.J. Self-organization and polyolefin nucleation efficacy of 1,3:2,4-di-p-methylbenzylidene sorbitol. *J. Polym. Sci. Part B Polym. Phys.* **1997**, *35*, 2617–2628. [[CrossRef](#)]
23. Smith, T.; Masilamani, D.; Bui, L.; Khanna, Y.; Bray, R.; Hammond, W.; Curran, S.; Belles, J.; Binder-Castelli, S. The Mechanism of Action of Sugar Acetals as Nucleating Agents for Polypropylene. *Macromolecules* **1994**, *27*, 3147–3155. [[CrossRef](#)]
24. Lin, M.C.; Chen, H.L.; Lin, W.F.; Huang, P.S.; Tsai, J.C. Crystallization of Isotactic Polypropylene under the Spatial Confinement Templated by Block Copolymer Microdomains. *J. Phys. Chem. B* **2012**, *116*, 12357–12371. [[CrossRef](#)] [[PubMed](#)]
25. Sukhanova, T.; Lednický, F.; Urban, J.; Baklagina, Y.; Mikhailov, G.; Kudryavtsev, V. Morphology of melt crystallized polypropylene in the presence of polyimide fibres. *J. Mater. Sci.* **1995**, *30*, 2201–2214. [[CrossRef](#)]
26. Abdou, J.; Braggini, G.; Luo, Y.; Stevenson, A.; Chun, D.; Zhang, S. Graphene-Induced Oriented Interfacial Microstructures in Single Fiber Polymer Composites. *Appl. Mater. Interfaces* **2015**, *7*, 13620–13626. [[CrossRef](#)] [[PubMed](#)]
27. Ponçot, M.; Martin, J.; Chaudemanche, S.; Ferry, O.; Schenk, T.; Bourson, P. Complementarities of high energy WAXS and Raman spectroscopy measurements to study the crystalline phase orientation in polypropylene blends during tensile test. *Polymer* **2015**, *80*, 27–37. [[CrossRef](#)]
28. Avrami, M. Kinetics of Phase Change. II Transformation-Time Relations for Random Distribution of Nuclei. *J. Chem. Phys.* **1940**, *8*, 212–224. [[CrossRef](#)]
29. Yi, Q.-F.; Wen, X.-J.; Niu, H.; Dong, J.-Y. How does a polymerized compounding affect the nucleation effect of a sorbitol derivative nucleating agent in isotactic polypropylene melt crystallization? *J. Appl. Polym. Sci.* **2013**, *127*, 888–903. [[CrossRef](#)]
30. Katsuno, S.; Yoshinaga, M.; Kitade, S.; Sanada, Y.; Akiba, I.; Sakurai, K.; Masunaga, H. Crystallization kinetics of polypropylene containing a sorbitol nucleating agent. *Polym. J.* **2013**, *45*, 87–93. [[CrossRef](#)]
31. Mi, D.; La, R.; Chen, W.; Zhang, J. Different kinds of transcrystallinity developed from glass fiber/isotactic polypropylene/ β -nucleation agents composite by microinjection molding. *Polym. Adv. Technol.* **2016**, *27*, 1220–1227. [[CrossRef](#)]
32. Amitay-Sadovsky, E.; Cohen, S.R.; Wagner, H.D. Nanoscale Shear and Indentation Measurements in Transcrystalline R-Isotactic Polypropylene. *Macromolecules* **2001**, *34*, 1252–1257. [[CrossRef](#)]

